Langmuir
Article
pubs.acs.org/Langmuir

Metal-Chelating and Dansyl-Labeled Poly(*N*-isopropylacrylamide) Microgels as Fluorescent Cu^{2+} Sensors with Thermo-Enhanced Detection Sensitivity

Jun Yin, Xuefeng Guan, Di Wang, and Shiyong Liu*

CAS Key Laboratory of Soft Matter Chemistry, Department of Polymer Science and Engineering, Hefei National Laboratory for Physical Sciences at the Microscale, University of Science and Technology of China, Hefei, Anhui 230026, China

Received April 18, 2009. Revised Manuscript Received July 5, 2009

We report on the fabrication of Cu^{2+}-sensing thermoresponsive poly(*N*-isopropylacrylamide) (PNIPAM) microgels labeled with metal-chelating acceptor and fluorescent reporter moieties. Cu^{2+} detection sensitivity can be considerably enhanced via thermo-induced collapse of the sensing matrix, which can easily optimize the relative spatial distribution of Cu^{2+}-binding sites and fluorescence readout functionalities. A novel picolinamine-containing monomer with Cu^{2+}-binding capability, *N*-(2-(2-oxo-2-(pyridine 2-yl-methylamino)ethylamino)ethyl)acrylamide (PyAM, **3**), was synthesized at first. Nearly monodisperse Cu^{2+}-sensing microgels were prepared via emulsion polymerization of *N*-isopropylacrylamide (NIPAM) in the presence of a nonionic surfactant, *N*,*N*′-Methylene-bis(acrylamide) (BIS), PyAM (**3**), and fluorescent dansylaminoethyl- acrylamide (DAEAM, **5**) monomers at around neutral pH and 70 °C. At 20 °C, as-synthesized microgels in their swollen state can selectively bind Cu^{2+} over other metal ions (Hg^{2+}, Mg^{2+}, Zn^{2+}, Pb^{2+}, Ag^{+}, and Al^{3+}), leading to prominent quenching of fluorescence emission intensity. Above the volume phase transition temperature, P(NIPAM-*co*-PyAM-*co*-DAEAM) microgels exhibit increased fluorescence intensity. It was observed that Cu^{2+} detection sensitivity can be dramatically enhanced via thermo-induced microgel collapse at elevated temperatures. At a microgel concentration of 3.0×10^{-6} g/mL, the detection limit drastically improved from ~46 nM at 20 °C to ~8 nM at 45 °C. The underlying mechanism for this novel type of sensor with thermotunable detection sensitivity was tentatively proposed.

Introduction

Chemosensors of heavy metal ions have received ever-increasing interest in the past decade due to their environmental and biological relevance.[1−20] Conventional small-molecule-based cation sensors consist of an ensemble of covalently linked ion-binding receptor and fluorophore reporter units, in which an ion-recognition event can be sensitively and selectively converted into easily detectable colorimetric or fluorescent signal changes.[21−39] In terms of fluorescent Cu^{2+} chemosensors, a quenching of fluorescence intensity was typically observed accompanied with ion binding. For instance, Kim et al.[40] developed

*To whom correspondence should be addressed. E-mail: sliu@ustc.edu.cn.

(1) Kim, J. S.; Quang, D. T. *Chem. Rev.* **2007**, *107*, 3780–3799.
(2) Lourdes, B. D.; David, N. R.; Mercedes, C. C. *Chem. Soc. Rev.* **2007**, *36*, 993–1017.
(3) Royzen, M.; Durandin, A.; Young, V. G.; Geacintov, N. E.; Canary, J. W. *J. Am. Chem. Soc.* **2006**, *128*, 3854–3855.
(4) Huang, F. H.; Jones, J. W.; Slebodnick, C.; Gibson, H. W. *J. Am. Chem. Soc.* **2003**, *125*, 14458–14464.
(5) Brummer, O.; La Clair, J. J.; Janda, K. D. *Org. Lett.* **1999**, *1*, 415–418.
(6) Wen, Z. C.; Yang, R.; He, H.; Jiang, Y. B. *Chem. Commun.* **2006**, 106–108.
(7) Kim, S. H.; Kim, J. S.; Park, S. M.; Chang, S. K. *Org. Lett.* **2006**, *8*, 371–374.
(8) Gunnlaugsson, T.; Leonard, J. P.; Murray, N. S. *Org. Lett.* **2004**, *6*, 1557–1560.
(9) Wu, Q. Y.; Anslyn, E. V. *J. Am. Chem. Soc.* **2004**, *126*, 14682–14683.
(10) Bag, B.; Bharadwaj, P. K. *Org. Lett.* **2005**, *7*, 1573–1576.
(11) Kramer, R. *Angew. Chem., Int. Ed.* **1998**, *37*, 772–773.
(12) Rurack, K.; Kollmannsberger, M.; Resch-Genger, U.; Daub, J. *J. Am. Chem. Soc.* **2000**, *122*, 968–969.
(13) Inoue, M. B.; Medrano, F.; Inoue, M.; Raitsimring, A.; Fernando, Q. *Inorg. Chem.* **1997**, *36*, 2335–2340.
(14) Ghosh, P.; Bharadwaj, P. K.; Mandal, S.; Ghosh, S. *J. Am. Chem. Soc.* **1996**, *118*, 1553–1554.
(15) Martinez-Manez, R.; Sancenon, F. *Chem. Rev.* **2003**, *103*, 4419–4476.
(16) deSilva, A. P.; Gunaratne, H. Q. N.; Gunnlaugsson, T.; Huxley, A. J. M.; McCoy, C. P.; Rademacher, J. T.; Rice, T. E. *Chem. Rev.* **1997**, *97*, 1515–1566.
(17) Czarnik, A. W. *Acc. Chem. Res.* **1994**, *27*, 302–308.
(18) Zeng, H. H.; Thompson, R. B.; Maliwal, B. P.; Fones, G. R.; Moffett, J. W.; Fierke, C. A. *Anal. Chem.* **2003**, *75*, 6807–6812.
(19) Beltramello, M.; Gatos, M.; Mancin, F.; Tecilla, P.; Tonellato, U. *Tetrahedron Lett.* **2001**, *42*, 9143–9146.
(20) Yang, H.; Liu, Z. Q.; Zhou, Z. G.; Shi, E. X.; Li, F. Y.; Du, Y. K.; Yi, T.; Huang, C. H. *Tetrahedron Lett.* **2006**, *47*, 2911–2914.
(21) Zheng, Y.; Orbulescu, J.; Ji, X.; Andreopoulos, F. M.; Pham, S. M.; Leblanc, R. M. *J. Am. Chem. Soc.* **2003**, *125*, 2680–2686.
(22) Royzen, M.; Dai, Z. H.; Canary, J. W. *J. Am. Chem. Soc.* **2005**, *127*, 1612–1613.
(23) Zeng, L.; Miller, E. W.; Pralle, A.; Isacoff, E. Y.; Chang, C. J. *J. Am. Chem. Soc.* **2006**, *128*, 10–11.
(24) Kim, H. N.; Lee, M. H.; Kim, H. J.; Kim, J. S.; Yoon, J. *Chem. Soc. Rev.* **2008**, *37*, 1465–1472.
(25) Martinez, R.; Espinosa, A.; Tarraga, A.; Molina, P. *Org. Lett.* **2005**, *7*, 5869–5872.
(26) Lee, M. H.; Kim, H. J.; Yoon, S.; Park, N.; Kim, J. S. *Org. Lett.* **2008**, *10*, 213–216.
(27) Suresh, M.; Ghosh, A.; Das, A. *Chem. Commun.* **2008**, 3906–3908.
(28) Xie, J.; Menand, M.; Maisonneuve, P.; Metivier, R. *J. Org. Chem.* **2007**, *72*, 5980–5985.
(29) Kaur, N.; Kumar, S. *Chem. Commun.* **2007**, 3069–3070.
(30) Qi, X.; Jun, E. J.; Xu, L.; Kim, S. J.; Hong, J. S. J.; Yoon, Y. J.; Yoon, J. Y. *J. Org. Chem.* **2006**, *71*, 2881–2884.
(31) Weng, Y. Q.; Yue, F.; Zhong, Y. R.; Ye, B. H. *Inorg. Chem.* **2007**, *46*, 7749–7755.
(32) Swamy, K. M. K.; Ko, S. K.; Kwon, S. K.; Lee, H. N.; Mao, C.; Kim, J. M.; Lee, K. H.; Kim, J.; Shin, I.; Yoon, J. *Chem. Commun.* **2008**, 5915–5917.
(33) Xiang, Y.; Tong, A. J.; Jin, P. Y.; Ju, Y. *Org. Lett.* **2006**, *8*, 2863–2866.
(34) Yu, M. X.; Shi, M.; Chen, Z. G.; Li, F. Y.; Li, X. X.; Gao, Y. H.; Xu, J.; Yang, H.; Zhou, Z. G.; Yi, T.; Huang, C. H. *Chem.—Eur. J.* **2008**, *14*, 6892–6900.
(35) Schuster, M.; Sandor, M. *Fresenius J. Anal. Chem.* **1996**, *356*, 326–330.
(36) Bhalla, V.; Kumar, R.; Kumar, M.; Dhir, A. *Tetrahedron* **2007**, *63*, 11153–11159.
(37) Lewis, W. G.; Magallon, F. G.; Fokin, V. V.; Finn, M. G. *J. Am. Chem. Soc.* **2004**, *126*, 9152–9153.
(38) Prodi, L. *New J. Chem.* **2005**, *29*, 20–31.
(39) Shao, N.; Zhang, Y.; Cheung, S. M.; Yang, R. H.; Chan, W. H.; Mo, T.; Li, K. A.; Liu, F. *Anal. Chem.* **2005**, *77*, 7294–7303.
(40) Jung, H. S.; Kwon, P. S.; Lee, J. W.; Kim, J. I.; Hong, C. S.; Kim, J. W.; Kim, J. S. *J. Am. Chem. Soc.* **2009**, *131*, 2008–2012.

a coumarin-based fluorogenic probe covalently attached with a metal ion-binding picolinamine unit, which can serve as a highly selective sensor for the detection of intracellular Cu^{2+} ions. Krämer et al.[41] reported the synthesis of *N*-2-methyl-pyridyl-*N*′-dansylethylenediamine and its Cu^{2+}-sensing capability via fluorescence quenching, and the detection of Cu^{2+} ions in the micromolar range can even be checked by the naked eye under UV irradiation. Qian et al.[42,43] designed and synthesized 1,8-naphthalimide-based colorimetric and fluorescent Cu^{2+} sensors on the basis the internal charge transfer (ICT) mechanism, in which multidentate picolinamine units were employed as the selective metal ion-binding motif.

In the above examples of Cu^{2+} chemosensors, multistep synthesis is typically required for the preparation of sensing ensemble comprising covalently linked receptor and fluorescence readout moieties. Recently, the concept of self-organization has been introduced to the field of ion-selective chemosensors by employing surfactant micelles,[44−46] silica nanoparticles,[38,47−52] and other functionalized substrates[53−58] as the sensing matrix, aiming to achieve functional cooperativity and adaptability. Tonellato et al.[44] reported the fabrication of sensing ensembles composed of lipophilic ligand *N*-decyl-glycylglycine, fluorescent dye (8-anilino-naphthalensulfonic acid, ANS), and cationic surfactant, cetyltrimethylammonium bromide (CTAB). Surfactant micelles can solubilize ligand and dye molecules within the hydrophobic core, and the selective binding of Cu^{2+} ions lead to the fluorescence quenching of ANS. Later on, they further synthesized Cu^{2+} ion-binding amphiphilic acceptor and avoided the use of CTAB surfactant.[45] The same research group also reported Cu^{2+} sensors based on silica nanoparticle surfaces functionalized with picolinamine and dansyl derivatives, serving as ion-binding acceptors and fluorescence reporters, respectively.[47] The organization of these two components at the nanoparticle surface afforded multivalent binding sites with an increased affinity for Cu^{2+} ions, and the binding of a single metal cation led to the quenching of up to ten surrounding dansyl residues. Thus, signal amplification was achieved via cooperative and collective effects. In another example, Larpent and co-workers[59,60] synthesized polystyrene latex particles (15−20 nm) covalently attached with cyclam ligands; after impregnation with BODIPY dye within nanoparticles, selective detection of Cu^{2+} can be realized via fluorescence quenching.

Scheme 1. Synthetic Routes Employed for the Preparation of Cu^{2+}-Binding *N*-(2-(2-Oxo-2-(pyridine-2-yl-methylamino)ethylamino)ethyl)acrylamide Monomer (PyAM, 3)

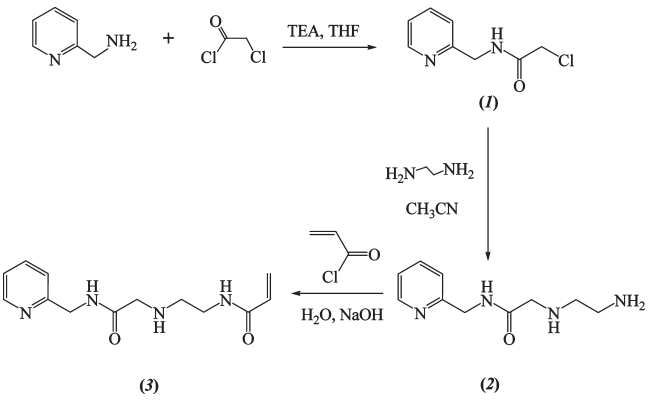

Compared to chromogenic and fluorogenic chemosensors based on the molecular-level host−guest recognition motif, self-organized chemosensors do not require the direct covalent linkage between receptor and fluorophore units, and their fabrication allows for the choice from a rich library of receptors and fluorescent dyes without extra synthetic works. It is noteworthy that the detection efficiency of self-organized chemosensors is closely dependent on the spatial arrangement of receptor and fluorescence reporter moieties within sensing ensembles.

It is well-known that thermoresponsive poly(*N*-isopropylacrylamide) (PNIPAM) microgels exhibit thermo-induced swelling/collapse behavior in aqueous dispersion, accompanied by considerable volume changes.[61−64] If the concept of self-organized chemosensors is applied to responsive microgels, we expect that the spatial arrangement of ion-binding acceptors and fluorescence reporter moieties can be easily tuned by external stimuli, such as pH and temperatures. Just recently, we reported a proof-of-concept example of microgel-based Cu^{2+} chemosensors by covalently incorporating polymerizable phenanthroline-containing fluorescent monomer (PhenUMA) into PNIPAM microgels. PhenUMA moieties are capable of simultaneous Cu^{2+}-binding and fluorescence sensing, and enhanced detection sensitivity upon thermo-induced microgel collapse has been achieved via the cooperative binding mechanism.[65] To test the general applicability of this novel designing principle, it is imperative to apply it to other microgel systems in which fluorescent reporters and ion chelators are spatially separated.

In this work, we synthesized thermoresponsive PNIPAM microgels copolymerized with ion-binding picolinamine-based residues (Scheme 1) and dansyl monomers. The detection sensitivity and selectivity of as-synthesized microgels to Cu^{2+} ions at varying temperatures were characterized in detail. We found that PNIPAM microgels could selectively bind Cu^{2+} over other metal ions, leading to prominent quenching of fluorescence emission

(41) Kovbasyuk, L.; Kramer, R. *Inorg. Chem. Commun.* **2006**, *9*, 586–590.
(42) Xu, Z. C.; Qian, X. H.; Cui, J. N. *Org. Lett.* **2005**, *7*, 3029–3032.
(43) Xu, Z. C.; Xiao, Y.; Qian, X. H.; Cui, J. N.; Cui, D. W. *Org. Lett.* **2005**, *7*, 889–892.
(44) Grandini, P.; Mancin, F.; Tecilla, P.; Scrimin, P.; Tonellato, U. *Angew. Chem., Int. Ed.* **1999**, *38*, 3061–3064.
(45) Berton, M.; Mancin, F.; Stocchero, G.; Tecilla, P.; Tonellato, U. *Langmuir* **2001**, *17*, 7521–7528.
(46) Mancin, F.; Rampazzo, E.; Tecilla, P.; Tonellato, U. *Chem.—Eur. J.* **2006**, *12*, 1844–1854.
(47) Rampazzo, E.; Brasola, E.; Marcuz, S.; Mancin, F.; Tecilla, P.; Tonellato, U. *J. Mater. Chem.* **2005**, *15*, 2687–2696.
(48) Arduini, M.; Marcuz, S.; Montolli, M.; Rampazzo, E.; Mancin, F.; Gross, S.; Armelao, L.; Tecilla, P.; Tonellato, U. *Langmuir* **2005**, *21*, 9314–9321.
(49) Brasola, E.; Mancin, F.; Rampazzo, E.; Tecilla, P.; Tonellato, U. *Chem. Commun.* **2003**, 3026–3027.
(50) Arduini, M.; Rampazzo, E.; Mancin, F.; Tecilla, P.; Tonellato, U. *Inorg. Chim. Acta* **2007**, *360*, 721–727.
(51) Montalti, M.; Prodi, L.; Zaccheroni, N.; Battistini, G.; Marcuz, S.; Mancin, F.; Rampazzo, E.; Tonellato, U. *Langmuir* **2006**, *22*, 5877–5881.
(52) Montalti, M.; Prodi, L.; Zaccheroni, N.; Falini, G. *J. Am. Chem. Soc.* **2002**, *124*, 13540–13546.
(53) Ding, L. P.; Cui, X. A.; Han, Y. N.; Lu, F. T.; Fang, Y. *J. Photochem. Photobiol. A: Chem.* **2007**, *186*, 143–150.
(54) Kim, Y. R.; Kim, H. J.; Kim, J. S.; Kim, H. *Adv. Mater.* **2008**, *20*, 4428–4432.
(55) Kim, H. J.; Lee, S. J.; Park, S. Y.; Jung, J. H.; Kim, J. S. *Adv. Mater.* **2008**, *20*, 3229+.
(56) Shang, L.; Dong, S. J. *J. Mater. Chem.* **2008**, *18*, 4636–4640.
(57) Lu, F. T.; Gao, L. N.; Ding, L. P.; Jiang, L. L.; Fang, Y. *Langmuir* **2006**, *22*, 841–845.
(58) Mu, L. M.; Shi, W. S.; Chang, J. C.; Lee, S. T. *Nano Lett.* **2008**, *8*, 104–109.
(59) Meallet-Renault, R.; Pansu, R.; Amigoni-Gerbier, S.; Larpent, C. *Chem. Commun.* **2004**, 2344–2345.
(60) Gouanve, F.; Schuster, T.; Allard, E.; Meallet-Renault, R.; Larpent, C. *Adv. Funct. Mater.* **2007**, *17*, 2746–2756.
(61) Horie, K.; Yamada, S.; Machida, S.; Takahashi, S.; Isono, Y.; Kawaguchi, H. *Macromol. Chem. Phys.* **2003**, *204*, 131–138.
(62) Pelton, R. *Adv. Colloid Interface Sci.* **2000**, *85*, 1–33.
(63) Berndt, I.; Richtering, W. *Macromolecules* **2003**, *36*, 8780–8785.
(64) Senff, H.; Richtering, W. *J. Chem. Phys.* **1999**, *111*, 1705–1711.
(65) Liu, T.; Hu, J. M.; Yin, J.; Zhang, Y. F.; Li, C. H.; Liu, S. Y. *Chem. Mater.* **2009**, DOI: 10.1021/cm901070a.

Scheme 2. (a) Synthetic Scheme Employed for the Preparation of Cu^{2+}-Sensing P(NIPAM-*co*-PyAM-*co*-DAEAM) Microgels via Emulsion Polymerization. (b) Schematic Illustration for P(NIPAM-*co*-PyAM-*co*-DAEAM) Microgel-Based Selective Cu^{2+} Detection via Fluorescence Quenching and the Enhancement of Detection Sensitivity via Thermo-Induced Microgel Collapse

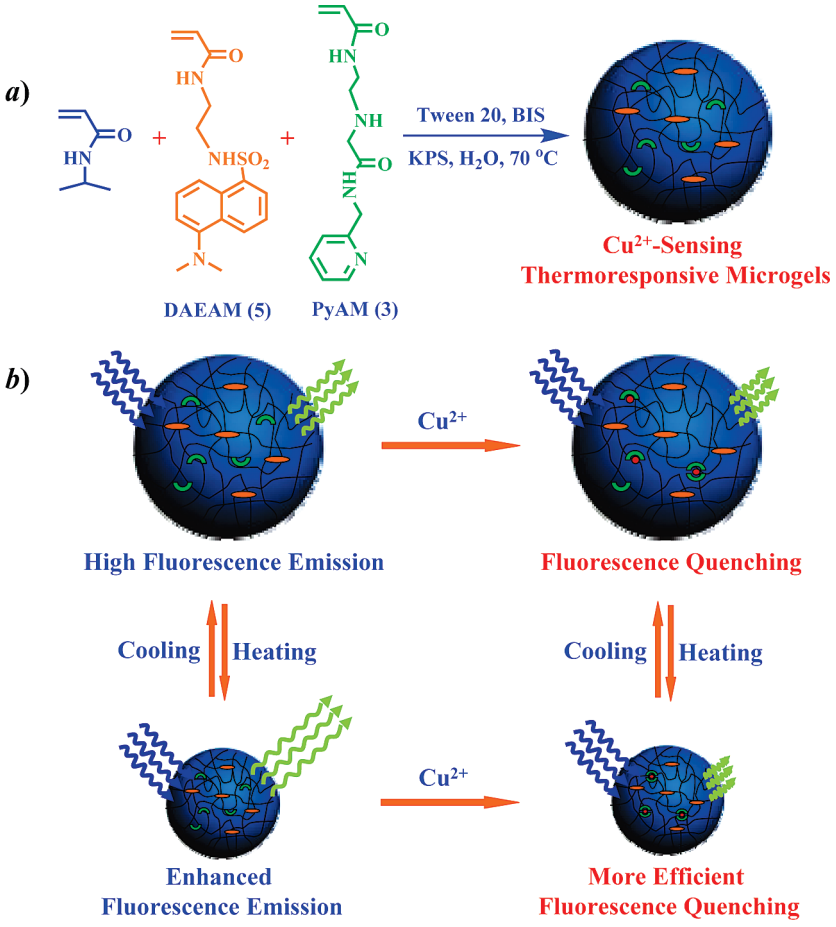

intensity of dansyl moieties. Moreover, Cu^{2+} detection sensitivity of microgels can be dramatically enhanced via thermo-induced microgel collapse at elevated temperatures (Scheme 2). The detection limit considerably improved from ~46 nM at 20 °C to ~8 nM at 45 °C with a microgel concentration of 3.0×10^{-6} g/mL.

Experimental Section

Materials. *N*-Isopropylacrylamide (NIPAM, 97%, Tokyo Kasei Kagyo Co.) was purified by recrystallization from a mixture of benzene and *n*-hexane (1/3, v/v). Dansyl chloride (98%, Acros), 2-(aminomethyl)pyridine (99%, Alfa Aesar), and chloroacetyl chloride (98%, Aldrich) were used as received. Acryloyl chloride (Sinopharm Chemical Reagent Co.) was distilled at reduced pressure just prior to use. Potassium persulfate (KPS) and *N,N′*-methylene-bis(acrylamide) (BIS) were recrystallized from methanol and ethanol, respectively, and stored at −20 °C prior to use. Nonionic surfactant, polyoxyethylene sorbitan monolaurate (Tween 20), was purchased from Amersco and used as received. Triethylamine (TEA) and 1,2-ethylenediamine were vacuum-distilled over CaH_2. Dichloromethane (CH_2Cl_2) and acetonitrile (MeCN) were dried over CaH_2 and distilled just prior to use. Methanol, tetrahydrofuran, ethyl acetate (EtOAc), ethylenediaminetetraacetic acid (EDTA), and all other chemicals were purchased from Sinopharm Chemical Reagent Co. Ltd. and used as received. Nitrate salts (Cu^{2+}, Pb^{2+}, Zn^{2+}, Ag^{+}, Mg^{2+}, Al^{3+}, and Hg^{2+}) were used for all sensing experiments. Water was deionized with a Milli-Q SP reagent water system (Millipore) to a specific resistivity of 18.4 MΩ cm.

Synthetic schemes employed for the preparation of *N*-(2-(2-oxo-2-(pyridine-2-yl- methylamino)ethylamino)ethyl)acrylamide (PyAM, **3**), dansylaminoethylacrylamide (DAEAM, **5**), and PNIPAM microgel sensors are shown in Schemes 1 and 2 and Scheme S1 in the Supporting Information.

Synthesis of 2-Chloro-N-(pyridin-2-yl-methyl)acetamide (***1***). 2-Chloro-*N*-(pyridin-2-yl-methyl)acetamide (**1**) was prepared according to literature procedures (Scheme 1).[47] Into a round-bottom flask equipped with a magnetic stirring bar, 2-(aminomethyl)pyridine (2.0 g, 18.5 mmol), TEA (2.82 mL, 19.5 mmol), and dry THF (20 mL) were charged. After cooling to 0 °C in an ice−water bath, chloroacetyl chloride (1.55 mL, 19.5 mmol) in 40 mL dry THF was added dropwise over 1 h. After stirring for another 4 h at room temperature, the reaction was essentially complete as monitored by TLC (EtOAc/MeOH = 9/1). After filtration, the filtrates were evaporated to dryness under reduced pressure. The residues were dissolved in 50 mL EtOAc and extracted with saturated $NaHCO_3$ solution (3 × 20 mL). After drying over anhydrous Na_2SO_4, the solvent was removed under reduced pressure, yielding a light brown oil (3.0 g, yield: 88%). ^{1}H NMR ($CDCl_3$, δ, ppm, TMS; Figure S1, *a*): 8.55 (d, 1H, J = 4.72 Hz, pyridyl proton), 7.84 (br, 1H, -CH_2NHCO-), 7.64 (m, 1H, J = 1.76 and 5.94 Hz, pyridyl proton), 7.21 (m, 2H, pyridyl protons), 4.57 (d, 2H, J = 5.01 Hz, pyridyl-CH_2NH-), 4.10 (s, 2H, -CH_2Cl).

Synthesis of 2-(2-Aminoethylamino)-N-(pyridin-2-yl-methyl)-acetamide (***2***). Into a round-bottom flask equipped with a magnetic stirring bar, 1,2-ethylenediamine (48.78 mL, 0.73 mol) in 70 mL dry MeCN was charged. After cooling to 0 °C in an ice−water bath, **1** (3.0 g, 16.25 mmol) in 30 mL dry MeCN was added dropwise over 1.5 h. After stirring for another 5 h at room temperature, the solvent and excess of 1,2-ethylenediamine were

removed under reduced pressure, the residues were further purified by silica gel column chromatography using MeOH/THF (1/2, v/v) as eluent, yielding a brown−yellow oil (2.03 g, yield: 60%). ^{1}H NMR ($CDCl_3$, δ, ppm, TMS; Figure S1, *b*): 8.33 (d, 1H, J = 4.34 Hz, pyridyl proton), 7.74 (t, 1H, J = 7.71 Hz, -CH_2N*H*CO-), 7.26 (m, 2H, pyridyl protons), 4.41 (d, 2H, J = 5.01 Hz, pyridyl-CH_2NH-), 3.24 (s, 2H, -CH_2Cl), 2.85 (t, 2H, J = 6.11 Hz, -CH_2C$H_2$$NH_2$), 2.69 (t, 2H, J = 6.18 Hz, -C$H_2$$CH_2NH_2$).

*Synthesis of N-(2-(2-Oxo-2-(pyridin-2-yl-methylamino)-ethylamino)ethyl)acrylamide (PyAM, **3**).* Into a round-bottom flask equipped with a magnetic stirring bar, **2** (2.0 g, 9.6 mmol) and aqueous NaOH solution (40 mL, 0.24 M) were charged. After cooling to 0 °C in an ice−water bath, acryloyl chloride (1.57 mL, 19.2 mmol) was slowly added over 10 min. After stirring for another 1 h at room temperature, the solvent was removed under reduced pressure, and the obtained brown oil was further purified by silica gel column chromatography using MeOH/THF (1/1, v/v) as the eluent, yielding a slightly brown−yellow oil (1.26 g, yield: 50%). ^{1}H NMR ($CDCl_3$, δ, ppm, TMS; Figure S1, *c*): 8.35 (d, 1H, J = 4.54 Hz, pyridyl proton), 7.73 (t, 1H, J = 7.82 Hz, -CH_2-N*H*CO-), 7.25 (m, 2H, pyridyl protons), 6.74 (m, 1H, -CO-C*H*=CH_2), 5.79 and 5.31 (dd, 2H, J = 11.8 and 17.8 Hz, -COC-H=CH_2), 4.41 (d, 2H, J = 5.42 Hz, pyridyl-CH_2NH-), 3.23 (s, 2H, -CH_2Cl), 3.09 (t, 2H, J = 6.32 Hz, -NHCH_2CH_2NH-), 2.95 (t, 2H, J = 6.27 Hz, -NHC$H_2$$CH_2$NH-). ^{13}C NMR ($CDCl_3$, δ, ppm, Figure S2): 156.23, 149.01, 138.63, 123.28, and 121.93 (pyridyl), 170.22 (-NH*C*OCH_2NH-), 168.86 (-*C*OCH=CH_2), 127.34 (-CO-*C*H=CH_2), 125.09 (-COCH=*C*H_2), 52.43 (-NHCO*C*H_2NH-), 47.46 (pyridyl- *C*H_2NH-), 44.29 (-NH*C*H_2CH_2NH-), and 42.05 (-NHCH_2*C*H_2NH-).

*Synthesis of 2-Dansylaminoethylamine (**4**).* 2-Dansylaminoethylamine (**4**) was prepared according to slightly modified literature procedures (Supporting Information Scheme S1).[66−68] Into a round-bottom flask equipped with a magnetic stirring bar, 1,2-ethylenediamine (55.6 mL, 0.83 mol) and dry THF (200 mL) were charged. After cooling to 0 °C in an ice−water bath, dansyl chloride (5.0 g, 18.5 mmol) in 50 mL dry THF was added dropwise over 1.5 h. After stirring for another 2 h at room temperature, NaOH aqueous solution (1.0 M, 50 mL) was added. After removing THF on a rotary evaporator, the aqueous phase was extracted with CH_2Cl_2 (3 × 80 mL). The combined organic phase was dried over anhydrous Na_2SO_4. After filtration and removal of the solvent, the residues were further purified by crystallization from benzene/hexane mixture, yielding light green needles (5.36 g, yield: 94%). ^{1}H NMR ($CDCl_3$, δ, ppm, TMS): 8.53 (d, 1H, J = 8.7 Hz, Ar*H*), 8.31 (d, 1H, J = 8.8 Hz, Ar*H*), 8.23 (d, 1H, J = 7.5 Hz, Ar*H*), 7.53 (m, 2H, Ar*H*), 7.17 (d, 1H, J = 7.6 Hz, Ar*H*), 3.05 (m, 2H, -C$H_2$$CH_2NH_2$), 2.90 (6H, -N(C$H_3$)$_2$), and 2.68 (m, 2H, -$CH_2CH_2$$NH_2$).

*Synthesis of Dansylaminoethylacrylamide (DAEAM, **5**).*[66−68] Into a round-bottom flask equipped with a magnetic stirring bar, **4** (5.3 g, 17.18 mmol), TEA (2.75 mL, 19.0 mmol), and dry CH_2Cl_2 (100 mL) were charged. After cooling to 0 °C in an ice−water bath, acryloyl chloride (1.55 mL, 19.0 mmol) in 20 mL dry CH_2Cl_2 was added dropwise over 1 h. After stirring for another 5 h at room temperature, the precipitates were removed by filtration. The filtrates were evaporated to dryness under reduced pressure, and the residues were further purified by silica gel column chromatography using ethyl acetate/hexane (1/1, v/v) as eluent, yielding a light green solid (5.07 g, yield: 85%). ^{1}H NMR ($CDCl_3$, δ, ppm, TMS; Supporting Information Figure S3, *a*): 8.54 (d, 1H, J = 8.9 Hz, Ar*H*), 8.23 (m, 2H, Ar*H*), 7.53 (m, 2H, Ar*H*), 7.17 (d, 1H, J = 7.9 Hz, Ar*H*), 6.47 (m, 1H, -COC*H*=CH_2), 5.75 and 6.26 (dd, 2H, J = 11.1 and 17.4 Hz, -COCH=CH_2), 3.38 (s, 2H, -CH_2-CH_2NHCO-), 3.07 (s, 2H, -C$H_2$$CH_2$NHCO-), 2.87 (s, 6H, -N(CH_3)$_2$). ^{13}C NMR ($CDCl_3$, δ, ppm; Figure S3, *b*): 153.12, 135.01, 130.51, 130.05, 129.71, 127.04, 126.81, 125.39, 123.49, and 115.21 (naphthalenyl), 163.88 (-*C*OCH=CH_2), 128.49 (-CO-*C*H=CH_2), 118.89 (-COCH=*C*H_2), 45.51 (-NH*C*H_2*C*H_2NH-), 41.01 (-N(*C*H_3)$_2$).

Preparation of P(NIPAM-co-DAEAM) Microgels. The control microgel sample was prepared via emulsion polymerization and detailed procedures are as follows. Into a 250 mL three-neck round-bottom flask equipped with a mechanical stirrer, reflux condenser, and a nitrogen gas inlet, NIPAM (0.95 g, 8.4 mmol), BIS (0.05 g, 0.32 mmol), Tween 20 (50 mg, 0.04 mmol), and deionized water (100 mL) were charged. After heating to 70 °C and degassing by bubbling with nitrogen for 30 min, KPS (25 mg, 94 μmol) dissolved in 1.0 mL deionized water was injected under mechanical stirring at 400 rpm. DAEAM monomer (14.1 mg, 41 μmol) in 2.0 mL acetone was then added dropwise over ∼5 min. The polymerization was conducted under stirring for 7 h. The dispersion was passed through glass wool in order to remove particulate matter and then dialyzed against deionized water for 5 days. Fresh deionized water was replaced approximately every 6 h.

Preparation of Cu^{2+}-Sensing P(NIPAM-co-PyAM-co-DAEAM) Microgels. Typical procedures employed for the synthesis of PNIPAM microgels labeled with DAEAM and PyAM with [PyAM]/[DAEAM] = 1/1 are as follows. Into a 250 mL three-necked round-bottom flask equipped with a mechanical stirrer, reflux condenser, and a nitrogen gas inlet, NIPAM (0.95 g, 8.4 mmol), BIS (0.05 g, 0.32 mmol), PyAM monomer (10.7 mg, 41 μmol), Tween 20 (50 mg, 0.04 mmol), and deionized water (100 mL) were charged. After heating to 70 °C and degassing by bubbling with nitrogen for 30 min, KPS (25 mg, 94 μmol) dissolved in 1.0 mL deionized water was injected under mechanical stirring at 400 rpm. DAEAM monomer (14.2 mg, 41 μmol) in 2.0 mL acetone was then added dropwise over ∼5 min. The polymerization was conducted under stirring for 7 h. The dispersion was passed through glass wool in order to remove particulate matter and then dialyzed against deionized water for 5 days. Fresh deionized water was replaced approximately every 6 h. Following similar procedures, the preparation of PNIPAM microgels with varying [PyAM]/[DAEAM] molar ratios (1/4, 1/2, and 2/1) and fixed amount of DAEAM (relative to that of NIPAM and BIS) were also prepared (Table 1).

Characterization. *Nuclear Magnetic Resonance Spectroscopy (NMR).* All NMR spectra were recorded on a Bruker AV300 NMR spectrometer (resonance frequency of 300 MHz for ^{1}H) operated in the Fourier transform mode. $CDCl_3$ and D_2O were used as the solvents.

Field-Emission Scanning Electron Microscope (FE-SEM). FE-SEM observations were conducted on a high-resolution JEOL JSM-6700 field-emission scanning electron microscopy. The samples for SEM observations were prepared by placing 10 μL of microgel solutions on copper grids successively coated with thin films of Formvar and carbon.

Laser Light Scattering (LLS). A commercial spectrometer (ALV/DLS/SLS-5022F) equipped with a multitau digital time correlator (ALV5000) and a cylindrical 22 mW UNIPHASE He−Ne laser (λ_0 = 632 nm) as the light source was employed for dynamic and static LLS measurements. Scattered light was collected at a fixed angle of 90° for duration of ∼10 min. Distribution averages and particle size distributions were computed using cumulants analysis and CONTIN routines. All data were averaged over three measurements.

Fluorescence Measurements. Fluorescence spectra were recorded using a RF-5301/PC (Shimadzu) spectrofluorometer. The temperature of the water-jacketed cell holder was controlled by a programmable circulation bath. The slit widths were set at 4 nm for excitation and 4 nm for emission. For all microgel-based Cu^{2+} sensing experiments, microgel concentrations are fixed at 3.0×10^{-6} g/mL.

(66) Shea, K. J.; Stoddard, G. J.; Shavelle, D. M.; Wakui, F.; Choate, R. M. *Macromolecules* **1990**, *23*, 4497–4507.
(67) Tong, Z.; Ren, B. Y.; Gao, F. *Polymer* **2001**, *42*, 143–149.
(68) Ren, B. Y.; Gao, F.; Tong, Z.; Yan, Y. *Chem. Phys. Lett.* **1999**, *307*, 55–61.

Table 1. Summary of Dynamic LLS Characterization Results Obtained for Swollen and Nonswollen Cu^{2+}-Sensing P(NIPAM-*co*-PyAM-*co*-DAEAM) Microgels in Aqueous Solution at Varying Temperatures

	20 °C		45 °C		
entry [a]	$\langle R_h \rangle$ (nm)[b]	μ_2/Γ^{2} [b]	$\langle R_h \rangle$ (nm)[b]	μ_2/Γ^{2} [b]	[PyAM]/[DAEAM]
1	135	0.10	41	0.06	0
2	122	0.09	39	0.02	1/4
3	136	0.11	42	0.05	1/2
4	138	0.08	44	0.04	1/1
5	128	0.12	40	0.07	2/1

[a] All microgel samples possess a cross-linking density of 5.0 wt % and the amount of DAEAM monomer in the feed recipe was fixed to be 1.42 wt % relative to the sum of NIPAM and BIS. [b] Intensity average hydrodynamic radius, $\langle R_h \rangle$, and polydispersity indices, μ_2/Γ^2, were determined by dynamic LLS, and the estimated error associated with each value is ±2 nm.

Results and Discussion

Synthesis of P(NIPAM-*co*-PyAM-*co*-DAEAM) Microgels. Synthetic routes employed for the preparation of PyAM (**3**) and DAEAM (**5**) monomers, P(NIPAM-*co*-DAEAM) and P(NIPAM-*co*-PyAM-*co*-DAEAM) microgels are described in Schemes 1 and 2 and Scheme S1 in the Supporting Information. The novel metal-chelating monomer, **3**, was prepared by reacting 2-(aminomethyl)pyridine with chloroacetyl chloride at first, followed by the condensation reaction with an excess of 1,2-ethylenediamine; finally, **3** was obtained by the amidation reaction of **2** with acryloyl chloride (Scheme 1). The chemical structure of **3** was confirmed by ^{1}H and ^{13}C NMR analysis (Figures S1−S2 in the Supporting Information). The fluorescent monomer, **5**, was prepared by the condensation reaction of dansyl chloride with an excess of 1,2-ethylenediamine, followed by the amidation reaction with acryloyl chloride (Scheme S1). The chemical structure of **5** was confirmed by ^{1}H and ^{13}C NMR analysis (Figure S3).

P(NIPAM-*co*-PyAM-*co*-DAEAM) microgels were synthesized via emulsion copolymerization of NIPAM, PyAM (**3**), and DAEAM (**5**) monomers in the presence of BIS and Tween 20 at around neutral pH and 70 °C. The amount of DAEAM monomer in the feed recipe was fixed to 1.42 wt % relative to the sum of NIPAM and BIS, whereas the amount of PyAM (**3**) was varied to synthesize P(NIPAM-*co*-PyAM-*co*-DAEAM) microgels with varying [PyAM]/[DAEAM] molar ratios. As-synthesized microgels were characterized by SEM and LLS, and the results are summarized in Table 1.

SEM images shown in Supporting Information Figure S4 revealed the presence of nearly monodisperse and spherical nanoparticles with an average diameter of ~130 nm. Figure 1 shows temperature-dependent changes of intensity-average hydrodynamic radius, $\langle R_h \rangle$, obtained for the aqueous dispersion of P(NIPAM-*co*-PyAM-*co*-DAEAM) microgels with [PyAM]/[DAEAM] = 1/1, as determined by dynamic LLS. Upon heating, $\langle R_h \rangle$ decreases from 138 nm at 20 °C to 44 nm at 45 °C, and prominent microgel collapse occurs at around ~32 °C. The inset in Figure 1 shows typical hydrodynamic radius distributions, $f(R_h)$, of microgels at 20 and 45 °C, yielding polydispersity indices, μ_2/Γ^2, of 0.08 and 0.04, respectively. Microgel sizes determined by dynamic LLS at 45 °C are in general agreement with those determined by SEM (Supporting Information Figure S4).

With P(NIPAM-*co*-PyAM-*co*-DAEAM) microgels with [PyAM]/[DAEAM] = 1/1 taken as an example, static LLS revealed an apparent molar mass, $M_{w,app}$, of 2.21×10^8 g/mol at 20 °C. Upon heating to 45 °C, microgels exhibit ~30.9 times of volume shrinkage. Assuming that PyAM and DAEAM moieties possess a uniform distribution within microgels, we can calculate that the

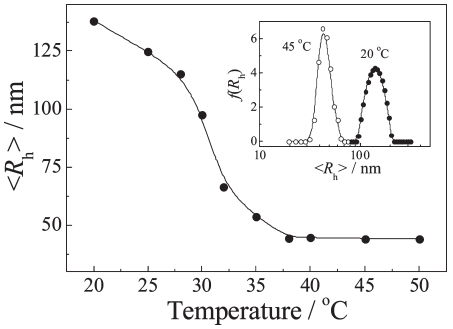

Figure 1. Temperature dependence of intensity average hydrodynamic radius, $\langle R_h \rangle$, obtained for the aqueous dispersion (3.0×10^{-6} g/mL) of P(NIPAM-*co*-PyAM-*co*-DAEAM) microgels with [PyAM]/[DAEAM] = 1/1. The inset shows typical hydrodynamic radius distributions, $f(R_h)$, of P(NIPAM-*co*-PyAM-*co*-DAEAM) microgels at 20 and 45 °C, respectively.

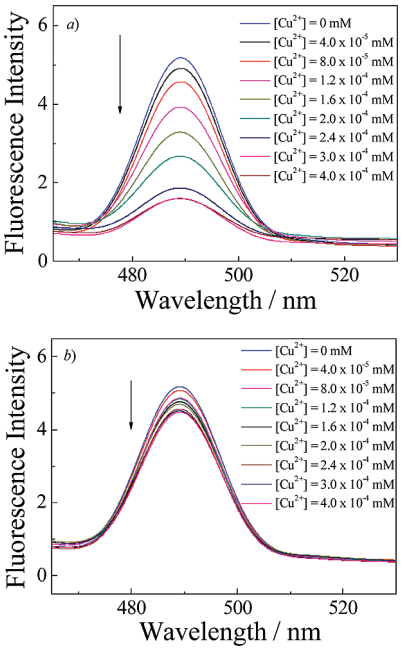

Figure 2. Fluorescence emission spectra (λ_{ex} = 420 nm; slit widths: Ex. 4 nm, Em. 4 nm) obtained for the aqueous dispersion (20 °C; pH 7, phosphate buffer; 3.0×10^{-6} g/mL) of (a) P(NIPAM-*co*-PyAM-*co*-DAEAM) ([PyAM]/[DAEAM] = 1/1, [PyAM] = 1.2×10^{-4} mM) and (b) P(NIPAM-*co*-DAEAM) microgels ([DAEAM] = 1.2×10^{-4} mM) upon gradual addition of Cu^{2+} ions.

average distance between neighboring PyAM and DAEAM moieties decreased from ~8.5 to 2.7 nm upon heating from 20 to 45 °C. We can expect that thermo-induced microgel collapse will enhance the formation of Cu^{2+}-PyAM complex with larger coordination numbers due to much closer spatial arrangement of PyAM residues; moreover, Cu^{2+} ions bound to PyAM acceptor should be able to more effectively quench the fluorescence emission of dansyl moieties due to that the relative distance between dansyl and PyAM residues are much closer within collapsed microgels relative to that in the swollen state.

P(NIPAM-*co*-PyAM-*co*-DAEAM) Microgel-Based Cu^{2+} Chemosensors. We then attempted to investigate the Cu^{2+}-sensing capability of P(NIPAM-*co*-PyAM-*co*-DAEAM) microgels in their swollen state at 20 °C. Typical fluorescence emission spectra (λ_{ex} = 420 nm) obtained for the aqueous dispersion (3.0×10^{-6} g/mL, [PyAM] = 1.2×10^{-4} mM) of P(NIPAM-*co*-PyAM-*co*-DAEAM) microgels ([PyAM]/[DAEAM] = 1/1) upon gradual

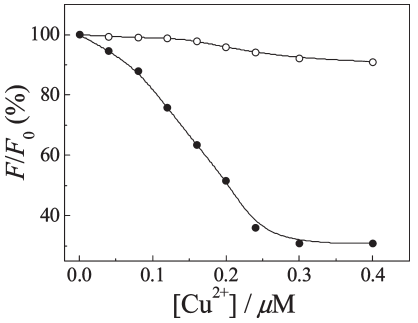

Figure 3. Change in relative fluorescence intensity (λ_{ex} = 420 nm, λ_{em} = 490 nm; slit widths: Ex. 4 nm, Em. 4 nm) recorded for aqueous dispersions (20 °C; pH 7, phosphate buffer; 3.0×10^{-6} g/mL) of (○) P(NIPAM-*co*-DAEAM) and (●) P(NIPAM-*co*-PyAM-*co*-DAEAM) microgels ([PyAM]/[DAEAM] = 1/1, [PyAM] = 1.2×10^{-4} mM) upon gradual addition of Cu^{2+} ions. F and F_0 represent fluorescence intensity of microgel chemosensors in the presence and absence Cu^{2+} ions, respectively.

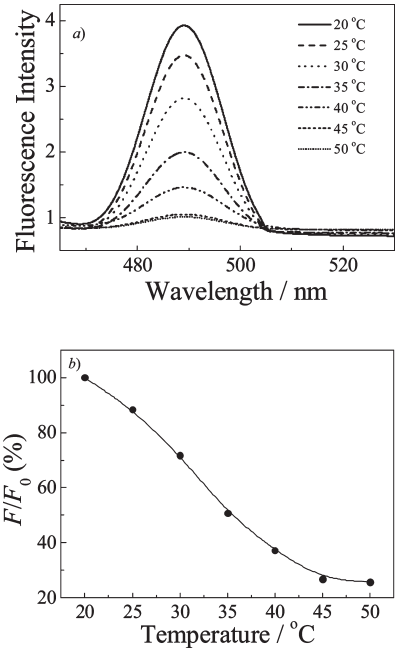

Figure 4. Temperature dependence of (a) fluorescence emission spectra (λ_{ex} = 420 nm, λ_{em} = 490 nm; slit widths: Ex. 4 nm, Em. 4 nm) and (b) change in relative fluorescence intensity recorded for the aqueous dispersion (pH 7, phosphate buffer; 3.0×10^{-6} g/mL) of P(NIPAM-*co*-PyAM-*co*-DAEAM) microgels ([PyAM]/[DAEAM] = 1/1, [PyAM] = 1.2×10^{-4} mM) upon addition of 1.0 equiv (1.2×10^{-4} mM) of Cu^{2+} ions. F and F_0 represent fluorescence intensity of microgel chemosensors at elevated temperatures and 20 °C, respectively.

addition of Cu^{2+} ions are shown in Figure 2a. Fluorescence intensity exhibits a prominent decrease upon Cu^{2+} addition and stabilizes over ~2.5 equiv of Cu^{2+} ions. As a control sample, the fluorescent intensity of P(NIPAM-*co*-DAEAM) microgels only show a slight decrease upon addition of Cu^{2+} up to ~3.3 equiv (Figure 2b).

The change in relative fluorescence intensity, F/F_0, for P(NIPAM-*co*-PyAM-*co*-DAEAM) and P(NIPAM-*co*-DAEAM) microgels upon gradual addition Cu^{2+} ions (0−0.4 μM) are summarized in Figure 3. Above 2.5 equiv of Cu^{2+} ions, fluorescence emission of the former decreases to ~30% of the initial value; i.e., a quenching efficiency of 70% was achieved. On the other hand, only a 10% decrease of fluorescence intensity is

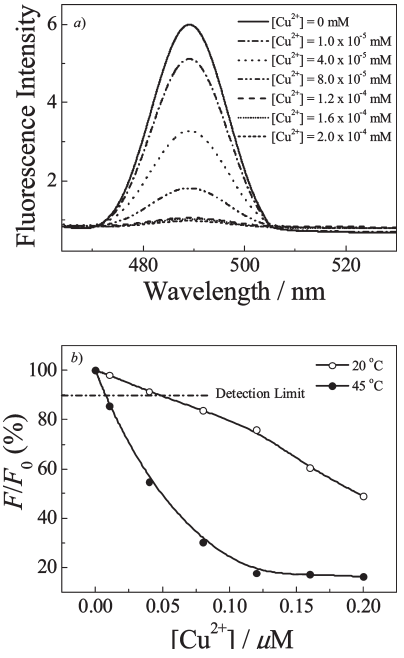

Figure 5. (a) Fluorescence emission spectra (λ_{ex} = 420 nm, λ_{em} = 490 nm; slit widths: Ex. 4 nm, Em. 4 nm) recorded for the aqueous dispersion (pH 7, phosphate buffer; 3.0×10^{-6} g/mL) of P(NIPAM-*co*-PyAM-*co*-DAEAM) microgels ([PyAM]/[DAEAM] = 1/1, [PyAM] = 1.2×10^{-4} mM) upon gradual addition of Cu^{2+} ions at 45 °C. (b) Change in relative fluorescence intensity of the aqueous dispersion of P(NIPAM-*co*-PyAM-*co*-DAEAM) microgels upon gradual addition of Cu^{2+} ions at 20 and 45 °C, respectively.

observed for P(NIPAM-*co*-DAEAM) microgels upon addition of 3.3 equiv Cu^{2+} ions. This indicates that PyAM ligands are necessary in the microgel recipes for the effective binding of Cu^{2+}; moreover, free Cu^{2+} ions do not exhibit appreciable fluorescence quenching of dansyl moieties.

Previously, Tonellato et al.[47] reported the fabrication of hybrid silica nanoparticles surface-functionalized with dansyl and picolinamine derivatives; Cu^{2+} detection limit can be down to ~30 nM. However, the detection can only be conducted in a water−DMSO mixture to ensure the solubility of functionalized silica nanoparticles. In the current work, P(NIPAM-*co*-PyAM-*co*-DAEAM) microgels are well-dispersible in water. Moreover, the thermoresponsiveness of PNIPAM-based microgels provides the advantage of easily tuning the relative distance between PyAM and DAEAM residues via the volume phase transition.

In the absence of Cu^{2+} ions, the fluorescence intensity of P(NIPAM-*co*-PyAM- *co*-DAEAM) microgels exhibit ~15% increase upon heating from 20 to 45 °C (Supporting Information Figure S5). This is understandable considering that fluorescent DAEAM residues are located in a hydrophobic environment in collapsed microgels.[69,70] In terms of Cu^{2+} sensing, the collapse of microgels at elevated temperatures provides three merits for the enhancement of detection sensitivity. First, the relative distance between metal-chelating PyAM moieties decreases, and this will result in the more efficient capture of Cu^{2+} ions via the cooperative complexation effects. Second, PyAM-Cu^{2+} complex will be able to effectively quench the fluorescence emission of surrounding dansyl residues due to their spatial closeness, as compared to swollen microgels. Finally, thermo-enhanced fluorescence

(69) Uchiyama, S.; Kawai, N.; de Silva, A. P.; Iwai, K. *J. Am. Chem. Soc.* **2004**, *126*, 3032–3033.
(70) Iwai, K.; Matsumura, Y.; Uchiyama, S.; de Silva, A. P. *J. Mater. Chem.* **2005**, *15*, 2796–2800.

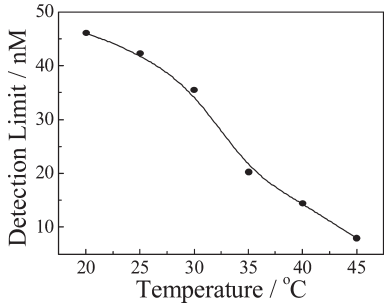

Figure 6. Temperature dependence of Cu^{2+} detection limits obtained for the aqueous dispersion (pH 7, phosphate buffer; 3.0×10^{-6} g/mL) of P(NIPAM-*co*-PyAM-*co*-DAEAM) microgels ([PyAM]/[DAEAM] = 1/1, [PyAM] = 1.2×10^{-4} mM).

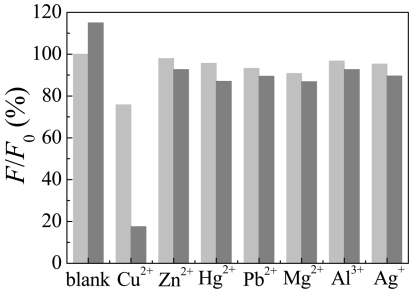

Figure 7. Selectivity of the aqueous dispersion (pH 7, phosphate buffer; 3.0×10^{-6} g/mL) of P(NIPAM-*co*-PyAM-*co*-DAEAM) microgels ([PyAM]/[DAEAM] = 1/1, [PyAM] = 1.2×10^{-4} mM) upon addition of 1.0 equiv (1.2×10^{-4} mM) of different metal ions at (a) 20 °C (light gray bars) and (b) 45 °C (dark gray bars), respectively. F and F_0 represent the fluorescence intensity (λ_{ex} = 420 nm, λ_{em} = 490 nm; slit widths: Ex. 4 nm, Em. 4 nm) of microgel dispersions in the presence and absence of metal ions, respectively. All experimental data were normalized with respect to F_0 of the microgel dispersion at 20 °C in the absence of metal ions.

emission of P(NIPAM-*co*-PyAM-*co*-DAEAM) microgels can provide more prominent signal changes during Cu^{2+}-sensing. In the next section, we will investigate the thermo-tunable detection sensitivity of P(NIPAM-*co*-PyAM-*co*-DAEAM) microgels to verify the above speculations.

Temperature-dependent changes in fluorescence intensity of P(NIPAM-*co*-PyAM-*co*-DAEAM) microgels in the presence of 1.0 equiv of Cu^{2+} are shown in Figure 4. We can clearly observe the dramatic decrease of fluorescence intensity in the temperature range 20−50 °C. Compared to that at 20 °C, the fluorescence quenching can be further improved for ~75% at 45 °C. This can be clearly ascribed to the decrease of relative distances between PyAM residues and between PyAM and DAEAM residues; the former leads to the formation of Cu^{2+}-PyAM complex with larger coordination numbers, and the latter leads to higher quenching efficiency.[47,71,72]

Figure 5a shows the fluorescence emission spectra recorded for the aqueous dispersion of P(NIPAM-*co*-PyAM-*co*-DAEAM) microgels upon gradual addition of Cu^{2+} ions at 45 °C. When comparing to that at 20 °C (Figure 2a), we can clearly judge that collapsed microgels at 45 °C exhibit considerably enhanced Cu^{2+}-sensing capability, as evidenced by the prominent decrease of fluorescence intensity (Figure 5a). Moreover, upon addition of ~1.0 equiv of Cu^{2+} ions, the fluorescence intensity tends to

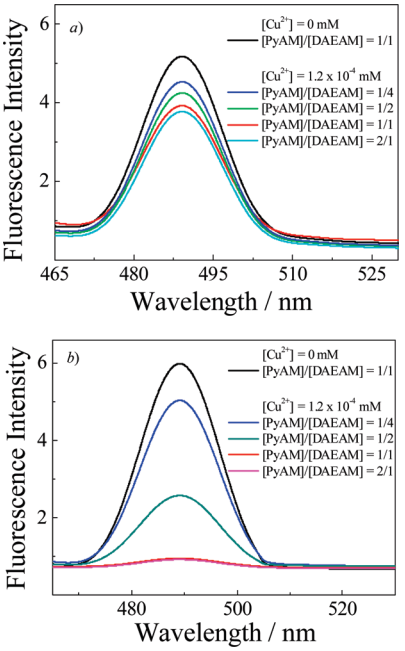

Figure 8. Fluorescence emission spectra (λ_{ex} = 420 nm, λ_{em} = 490 nm; slit widths: Ex. 4 nm, Em. 4 nm) recorded for the aqueous dispersion (pH 7, phosphate buffer; 3.0×10^{-6} g/mL) of P(NIPAM-*co*-PyAM-*co*-DAEAM) microgels ([DAEAM] = 1.2×10^{-4} mM) with varying [PyAM]/[DAEAM] molar ratios upon addition of a fix amount of Cu^{2+} ions (1.2×10^{-4} mM) at (a) 20 °C and (b) 45 °C, respectively.

stabilize, suggesting that all PyAM moieties have participated in the formation of the Cu^{2+}-PyAM complex. If we define the detection limit as the Cu^{2+} concentration at which a 10% fluorescence quenching can be measured by employing 3.0×10^{-6} g/mL aqueous dispersion of P(NIPAM-*co*-PyAM-*co*-DAEAM) microgels with [PyAM]/[DAEAM] = 1/1, the Cu^{2+} detection limit considerably improves from ~46 nM to ~8 nM upon a temperature increase from 20 to 45 °C (Figure 5b). Figure 6 shows the temperature-dependent detection limits for Cu^{2+} ions. We can conclude that the Cu^{2+} detection limits monotonically decrease with increase in detection temperature. Moreover, the most prominent decrease of detection limits occurs at around the volume phase transition temperature (~32 °C) of microgels (Figure 1). The stopped-flow technique was then employed to investigate the time period required for fluorescence detection upon addition of Cu^{2+} ions (Supporting Information Figure S6). We can see that, at 25 and 45 °C, ~5 and 10 s are required for the fluorescence intensity to reach equilibrium values. As longer equilibration time is needed at elevated temperatures, we propose that the detection process is diffusion-controlled. At 45 °C, the collapse of microgels renders the diffusion of Cu^{2+} ions into gel networks more difficult, as compared to the swollen state at 25 °C.

We further investigate the detection selectivity of P(NIPAM-*co*-PyAM-*co*-DAEAM) microgels to Cu^{2+} ions, as compared to other metal ions, such as Hg^{2+}, Mg^{2+}, Zn^{2+}, Pb^{2+}, Ag^{+}, and Al^{3+} (Supporting Information Figure S7 and Figure 7). At 20 °C, the additional 1.0 equiv of Cu^{2+} ions exhibits the most prominent fluorescence quenching efficiency (~24%) compared to other metal ions (Figure S7, *a*). This indicates that the incorporation of picolinamine moieties into PNIPAM microgels does not alter their Cu^{2+}-binding capability. Most importantly, the selectivity to Cu^{2+} ions can be further improved if the detection was conducted at 45 °C (Figure S7, *b*). Figure 7 summarizes the selectivity of P(NIPAM-*co*-PyAM-*co*-DAEAM) microgels to Cu^{2+} ions at

(71) Sigel, H.; Martin, R. B. *Chem. Rev.* **1982**, *82*, 385–426.
(72) Tsuboyama, B. S.; Sakurai, T.; Kobayashi, K. *Acta Crystallogr.* **1984**, *B40*, 466–473.

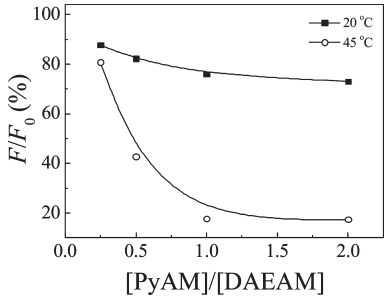

Figure 9. Change in relative fluorescence intensity ($\lambda_{ex} = 420$ nm, $\lambda_{em} = 490$ nm; slit widths: Ex. 4 nm, Em. 4 nm) recorded for the aqueous dispersion (pH 7, phosphate buffer; 3.0×10^{-6} g/mL) of P(NIPAM-*co*-PyAM-*co*-DAEAM) microgels ([DAEAM] = 1.2×10^{-4} mM) with varying [PyAM]/[DAEAM] molar ratios upon addition of a fix amount of Cu^{2+} ions (1.2×10^{-4} mM) at (a) 20 °C and (b) 45 °C, respectively. F_0 represents fluorescence intensity of microgel chemosensors ([PyAM]/[DAEAM] = 1/1, [PyAM] = 1.2×10^{-4} mM) at 20 °C in the absence of any metal ions.

20 and 45 °C, respectively. In the presence of other metal ions such as Zn^{2+}, Hg^{2+}, Pb^{2+}, Mg^{2+}, Al^{3+}, and Ag^{+}, P(NIPAM-*co*-PyAM-*co*-DAEAM) microgels also exhibit excellent selectivity to Cu^{2+} (Supporting Information Figure S8). The current system also provides detection reversibility. As shown in Supporting Information Figure S9, the addition of EDTA into the aqueous mixture of microgels and Cu^{2+} ions can almost recover the fluorescence emission intensity to that of the blank microgel dispersion in the absence of Cu^{2+} ions. This is reasonable considering that the Cu^{2+}-EDTA complex will form, which is accompanied by the disruption of the Cu^{2+}-PyAM complex. In principle, after removing the Cu^{2+}-EDTA complex via dialysis, the obtained microgel dispersion could be reused for Cu^{2+} sensing.

The molar ratio between PyAM acceptors and DAEAM dye within PNIPAM microgels can also considerably affect the detection sensitivity of Cu^{2+} ions. Figure 8 shows the fluorescence emission spectra recorded for the aqueous dispersion P(NIPAM-*co*-PyAM-*co*- DAEAM) microgels with varying [PyAM]/[DAEAM] molar ratios in the presence of 1.0 equiv of Cu^{2+} ions. In agreement with previous results (Figures 4 and 5), the quenching efficiency can be improved for all [PyAM]/[DAEAM] ratios by elevating the detection temperatures (Figure 9). However, it turns out that Cu^{2+} detection capability of microgels can be optimized at [PyAM]/[DAEAM] = 1/1, and further increasing the molar ratios does not help improve the detection sensitivity.[47]

Conclusion

In summary, we report on the synthesis of thermoresponsive PNIPAM microgel-based Cu^{2+} chemosensors by the incorporation of picolinamine-based acceptors (PyAM) and fluorescent reporters (DAEAM). At 20 °C, as-synthesized microgels in their swollen state can selectively bind Cu^{2+} over other metal ions (Hg^{2+}, Mg^{2+}, Zn^{2+}, Pb^{2+}, Ag^{+}, and Al^{3+}), leading to prominent quenching of fluorescence emission intensity. Most importantly, the detection sensitivity of P(NIPAM-*co*-PyAM-*co*-DAEAM) microgels can be further enhanced via thermo-induced microgel collapse at elevated temperatures. At a microgel concentration of 3.0×10^{-6} g/mL, Cu^{2+} detection limits considerably improve from ~46 nM to ~8 nM upon elevating detection temperatures from 20 to 45 °C. Microgels provide to be a robust platform to develop water-dispersible sensors with enhanced detection sensitivity by combining the concept of self-organized chemosensors with stimuli-responsive soft matter entities.

Acknowledgment. The financial supports of National Natural Scientific Foundation of China (NNSFC) Projects (20534020, 20674079, and 20874092), Specialized Research Fund for the Doctoral Program of Higher Education (SRFDP), and the Program for Changjiang Scholars and Innovative Research Team in University (PCSIRT) are gratefully acknowledged.

Supporting Information Available: Additional information as described in the text. This material is available free of charge via the Internet at http://pubs.acs.org.